

On the optical thickness dependence of the electro-optical properties of an in-plane switching LC cell

T. BEICA, S. FRUNZA^{*}, I. ZGURA, R. MOLDOVAN^a, A. DINESCU^b

National Institute of Materials Physics, R-077125 Magurele, Romania

^aRomanian Academy Center for Advanced Studies in Physics, R-050711 Bucharest, Romania

^bNational Institute of Microtechnologies, R-077190 Bucharest, Romania

The optical transmission of a liquid crystal cell with in-plane switching (IPS) mode is studied as function of the thickness for different rubbing angles and anchoring energy. It was found that the light transmission has a maximum at the value of ~ 0.66 for the ratio of the optical path difference (introduced by the undisturbed cell) to λ and that this value does not depend on λ , in the case of a very strong anchoring energy and of a rubbing angle of 13° . These experimental results agree very well with simulations using a simplified model. Moreover, the simulations have shown that the thickness corresponding to such a maximum optical path difference depends non-monotonously on the anchoring strength for five values of the rubbing angles (in the range 0 to 40°). For a given anchoring energy this thickness decreases with increasing rubbing angle.

(Received February 18, 2008; accepted March 12, 2008)

Keywords: Electro-optical properties, IPS cell, Anchoring energy, Optical thickness, Simulation of transmission curves

1. Introduction

The study of the electro-optical properties of liquid crystals (LCs) led in last decades to a variety of liquid crystal displays operating on the base of different principles. Among them twisted nematic and super-twisted nematic were the most used. The main disadvantage of these devices lies on the limiting viewing characteristics.

A solution to overcome this drawback was proposed as the in-plane switching mode [1]. Inherent wide viewing angle properties of this operating mode attracted an increasing interest [2-12] in the investigation of electro-optical properties as well as of some technological issues.

As it is well known in a liquid crystal display operating in the IPS mode the liquid crystal is submitted to an electric field parallel to the plane of the substrates. The electric field is produced by the voltage applied to the electrode stripes deposited on the surface of one of the plates. Usually in the "off state" the liquid crystal is homogeneously aligned. In the "on state", the voltage applied to the electrodes produces an in-plane electric field, which twists the liquid crystal, the molecules remaining in planes parallel to the substrate. To obtain a black mode the polarizer axis is parallel to the easy axis of the substrates and the analyzer is crossed.

In this paper we report on the thickness dependence of the optical transmission of the IPS liquid crystal cell for different rubbing angles and different anchoring energies. In the case of a very strong anchoring energy and of a rubbing angle of 13° , the measured light transmission as function of the ratio of the optical path difference introduced by the undisturbed cell to λ (the wave length of the light used in the measurement) has a maximum at 0.66 , which does not depend on λ . We called the liquid crystal thickness, which determines such an optical path difference as optimum thickness. These experimental

results agree very well with our results obtained by simulation with a simplified model. Additional simulations were performed to put in evidence the dependence of the optimum thickness on anchoring strength for five values of the rubbing angles covering the range between 0° and 40° . It was found that the optimum thickness has a non-monotonous dependence of the anchoring strength. For a given anchoring energy the optimum thickness decreases with increasing rubbing angle.

2. Experimental

IPS liquid crystal cell. Thickness of the liquid crystal layer is one of the parameters, which significantly influences the electro-optical characteristics of the LC cells and usually has the value of a few μm , difficult to be ensured without assembling of the cell in a clean room. The use of a cell having a plan-convex lens as one of the cell plates can be a way to overcome the lack of clean room conditions.

The experimental cell used in our experiments (sketched in Fig. 1) has as main parts one glass plate supporting the electrode stripes and a one plan-convex lens with the convex surface toward the cell interior. The lens is fixed on a T-shaped support (A); some screws allow a fine tune of the apex position of the lens so that a desired distance to the IDE glass plate is reached while the apex is on the optical axis of the measurement set-up. The glass plate with inter-digital electrodes (IDEs) is supported on the metal plate B; it was obtained from chromium deposited glass plates by photolithography. IDE configuration has the following features: electrode width is $50 \mu\text{m}$; the distance between the two neighboring electrodes is $10 \mu\text{m}$.

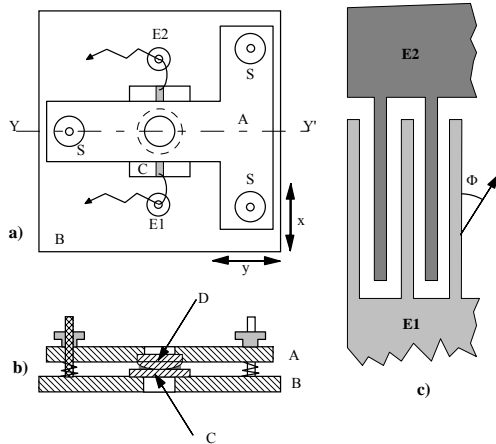


Fig. 1. Schematic view of the experimental cell: a) top view; b) section $Y - Y'$; c) detail of the IDE electrodes area with A – lens support; B – support of the IDE plate (with xy translation); C – IDE plate; D – lens; $E1$, $E2$ – electric connections and lock of IDE plate; S – adjustment screws and nuts. Φ – angle between rubbing direction and electrode stripes. The liquid crystal is placed between the lens and IDE plate.

Alignment films were deposited by spinning at 3000 rpm a polyvinyl alcohol (PVA) solution in water (1.5% wt); afterward the plates were thermally treated at 120°C for half an hour. To impose an easy axis for the liquid crystal alignment, the PVA films were unidirectionally rubbed at Φ degrees referenced to IDEs.

Liquid crystal to fill in the cell was 4-n-pentyl-cyanobiphenyl (5CB) from Aldrich and the filling was performed in the isotropic phase. Cooling in nematic phase results in a homogeneous LC cell in which the director orientation makes an established angle Φ with the electrode stripes (Fig. 1c).

The thickness H of the liquid crystal layer cannot be directly determined in our experimental set-up. Instead of H one can measure the optical path difference introduced by LC layer $\delta_\lambda = H\Delta n/\lambda$ expressed in wavelength λ of the monochromatic light, Δn representing the birefringence of LC at the wavelength λ . The temperature in the measuring chamber was kept at $26 \pm 0.5^\circ \text{C}$, the errors in evaluation of the LC thickness being less than $\pm 1\%$. The optical path difference δ_G for wavelength $\lambda = 548 \text{ nm}$ was measured using a tilting compensator (TC in Fig. 2).

Optical transmission measurements were performed using the set-up sketched in Fig. 2. The light source is a bulb and the interference filters B (488 nm), G (548 nm) or O (591 nm) allowed the measurements in monochromatic light. The polarizer P and the analyzer A ensured the choice of the operating mode of the cell. Intensity of the transmitted light was detected by the photomultiplier PM and its response was converted into a digital signal by an acquisition module (Axiom AX5411).

A sinusoidal voltage of the frequency of 1kHz was applied for registration of the transmission curves while its

root mean square (rms) value (measured with a digital voltmeter Keithley 2000) was varied at a rate less than 0.1 V/s.

The diameter of the investigated region was of about 0.4 mm around the apex of the spherical surface of the lens to ensure a good uniformity of the thickness of the LC layer.

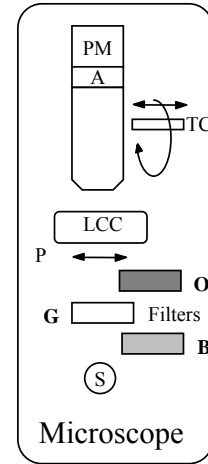


Fig. 2. Measuring set-up: S – bulb; B , G , O – interference filters; P – polarizer; LCC – LC cell; TC – tilting compensator; A – analyzer; PM – photomultiplier.

The light transmission as function of the rms value of applied voltage U was evaluated by the formula:

$$T(U) = \frac{I(U) - I_0}{I_1 - I_0} \quad (1)$$

where I_1 is the intensity of the light transmitted by the cell when the polarizer and the analyzer have their axes parallel to the orientation of the LC in the absence of electric field; I_0 is the intensity of the light transmitted by the cell when the polarizer is parallel to the LC orientation while the analyzer is perpendicular to that orientation; $I(U)$ is the intensity of the light transmitted by the cell submitted to an applied voltage U . According to this equation the transmission takes values in the interval 0 - 1.

3. Results and discussion

This section contains the experimental values obtained for transmission under different conditions and the curves simulated using a simple model as well.

3.1 Experimental transmission curves

In Fig. 3 (a, b, c) the dependence of the light transmission on the applied voltage for several values of optical path difference δ_G is shown for three wavelengths of the incident beam, respectively for 488 nm, 548 nm and 591 nm.

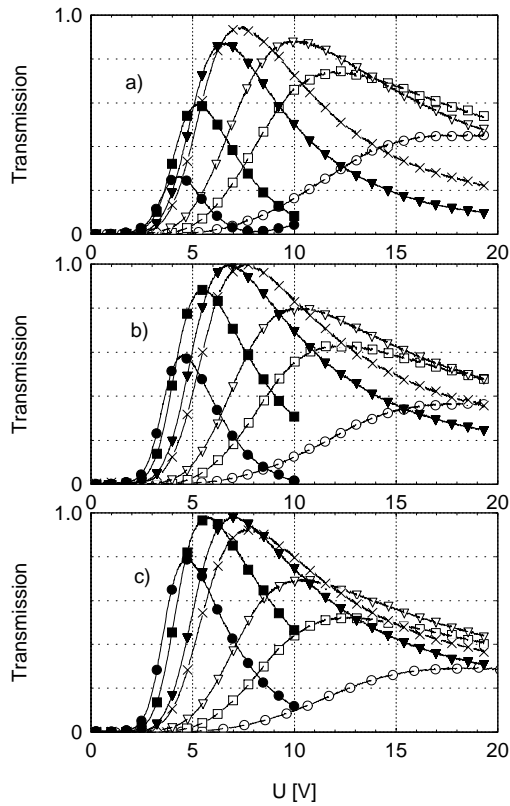


Fig. 3. Transmission of the cell as function of applied voltage at the chosen wavelengths: a) 488 nm, b) 548 nm and c) 591 nm. The layer thickness δ_G has the values: 0.28 (\circ); 0.38 (\square); 0.458 (∇); 0.597 (\times); 0.682 (\blacktriangledown); 0.824 (\blacksquare); 0.988 (\bullet).

From these figures one extracts the value of the maximum transmission corresponding to each of the optical path difference used in experiments. The data are displayed in Fig. 4, where each curve represents the dependence of the maximum value of the light transmission on the optical path difference for a given wavelength of the incident light beam.

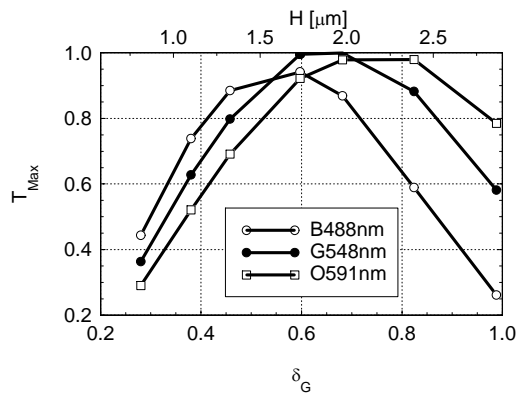


Fig. 4. Maximum transmission as function of the optical path difference δ_G for the chosen wavelengths.

The upper abscissa in Fig. 4 gives the LC thickness. It is possible to transform each of these curves by taking into account the optical path difference corresponding to the specified wavelength.

The birefringence of 5CB for the three wavelengths was obtained from the literature data [13] by interpolation; these values are as follows:

$$\begin{aligned} \Delta n(489\text{nm}) &= 0.2020 \\ \Delta n(548\text{nm}) &= 0.1891 \\ \Delta n(591\text{nm}) &= 0.1831 \end{aligned} \tag{2}$$

Therefore we have written the relationship:

$$\delta_\lambda = \frac{\Delta n(\lambda)}{\Delta n(548)} \cdot \frac{548}{\lambda} \delta_G \tag{3}$$

Using this relationship we find for each wavelength the dependence of the maximum of the light transmission on its own optical path difference δ_λ expressed in the adequate wavelength. The result of those transformations is shown in Fig. 5.

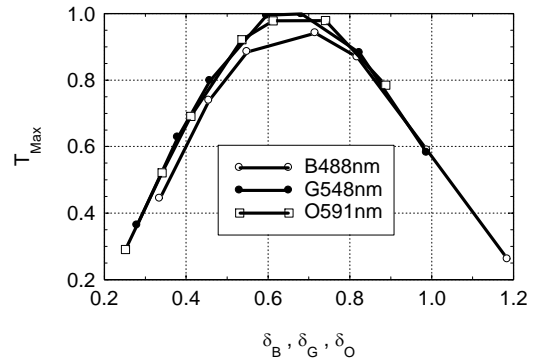


Fig. 5. Maximum transmission as function of the optical path difference for the used wavelengths $\lambda=448$ nm, 548 nm and 591 nm.

The maximum of the light transmission is reached for a value of the optical path difference expressed in $\delta_\lambda = H\Delta n(\lambda)/\lambda$ units equal to ~ 0.66 , which is the same for all the three wavelengths.

3.2 Simulation of transmission curves

The first step in the simulation of the transmission curves consists in the calculation of the director distribution in the IPS cell under an applied voltage U . We have used a very simple model [3], which assumes the following:

- The LC with positive dielectric anisotropy is uniformly oriented in the absence of an applied voltage and the nematic director makes an angle Φ with the OX axis, which is parallel to the electrode stripes.
- The electric field in the cell is uniform and is simply written as $E = U/d$, where U is the applied voltage and d is the distance between ID electrodes.
- The glass plate (so-called the command plate) with

ID electrodes is considered at $z = 0$ and is characterized by an azimuthal anchoring energy, which can take values between 0 and ∞ . For the reference plate situated at $z = H$ the azimuthal anchoring energy is a strong one.

- Within the cell everywhere in the plane $z = \text{const.}$, the azimuthal angle $\phi(z)$ has the same value.

- Azimuthal anchoring energy is given by a Rapini–Papoular type expression $F_S = \frac{1}{2}W_S \sin^2(\phi_0 - \Phi)$ where W_S is the anchoring energy coefficient and ϕ_0 is the angle at $z = 0$.

- The polarizer axis is parallel to the LC orientation in the cell without an applied voltage. The analyzer is crossed with the polarizer.

Starting with these hypotheses one computes the director distribution by minimizing the free energy per surface unit F :

$$F = \int_0^H \left[\frac{1}{2}K_{22} \left(\frac{\partial \phi}{\partial z} \right)^2 - \frac{\Delta \varepsilon}{2} E^2 \sin^2 \phi \right] dz - \frac{1}{2}W_S \cos^2(\phi_0 - \Phi) \quad (4)$$

K_{22} is the elastic twist constant; $\Delta \varepsilon$ is dielectric anisotropy. Making some substitutions dimensionless Euler – Lagrange equation is obtained

$$\frac{\partial^2 \phi}{\partial \zeta^2} + \frac{\xi_F^2}{2} \sin 2\phi = 0 \quad (5)$$

along with the boundary conditions:

$$\phi|_{\zeta=0} = \begin{cases} \Phi & \text{for strong anchoring} \\ \frac{\xi_S}{2} \sin 2(\phi|_{\zeta=0} - \Phi) & \text{for weak anchoring} \end{cases} \quad (6)$$

$$\frac{\partial \phi}{\partial \zeta} \Big|_{\zeta=1} = \Phi \quad (7)$$

where $\zeta = z/H$ is a reduced coordinate; $\xi_F = U(H/d)\sqrt{\varepsilon_0 \Delta \varepsilon / K_{22}}$ is a dimensionless field parameter, $\varepsilon_0 = 8.85 \cdot 10^{-12} \text{C}^2 \text{N}^{-1} \text{m}^{-2}$ is the vacuum permittivity and $\xi_S = W_S H / K_{22}$ is a dimensionless anchoring parameter.

A distance between electrodes of $10 \mu\text{m}$ was considered. The values corresponding to 5CB were introduced such as $K_{22} = 4 \text{pN}$ [14], $\Delta \varepsilon = 11.5$ [15].

The numerical integration of eq. (5) with the boundary conditions (6) and (7) was performed using a Runge – Kutta method and gives the values of the azimuthal angle ϕ_k and its derivative $\partial \phi_k / \partial \zeta$ in $N+1$ planes at $\zeta_k = k/N$ (with $k = 0, 1, \dots, N$).

The distorted LC in the IPS liquid crystal cell was considered as a stack of $N+1$ uniaxial homogeneous layers of thickness $h = H/N$ centered at z_k ($k = 1 \dots N-1$) and having the orientation given by

azimuthal angle $\phi'_k = \phi_k - \Phi$. Additionally, one takes into consideration two other layers with the thickness $h' = h/2$: the first one is placed in front of the stack at $z_0 = 0$ with the orientation $\phi'_0 = \phi_0 - \Phi$ and the second layer placed at the stack rear with $z_N = H$ and the orientation $\phi'_N = 0$.

We made the following additional assumptions:

- The incident light beam is normal to the entry polarizer and has the intensity equal to 1.

- The losses due polarizer and interfaces are neglected.

- The matrices characterizing the polarizer and the analyzer are $\begin{pmatrix} 1 \\ 0 \end{pmatrix}$ and $\begin{pmatrix} 0 & 1 \end{pmatrix}$ respectively.

In these conditions the transmission of the IPS cell can be written as

$$T = \left| \begin{pmatrix} 0 & 1 \end{pmatrix} \hat{M} \begin{pmatrix} 1 \\ 0 \end{pmatrix} \right|^2 \quad (8)$$

with the final Jones matrix $\hat{M} = \prod_{k=0}^N \hat{M}_k$, where Jones

matrix \hat{M}_k [16, 17] is the transfer matrix of the layer k and it is given by

$$\hat{M}_k \sim \begin{pmatrix} \cos \phi'_k & -\sin \phi'_k \\ \sin \phi'_k & \cos \phi'_k \end{pmatrix} \begin{pmatrix} e^{-i\alpha} & 0 \\ 0 & e^{i\alpha} \end{pmatrix} \begin{pmatrix} \cos \phi'_k & \sin \phi'_k \\ -\sin \phi'_k & \cos \phi'_k \end{pmatrix} \quad (9)$$

having

$$\alpha = \frac{2\pi n_e - n_o}{\lambda} h' \text{ for } k = 0 \text{ and } N$$

$$\alpha = \frac{2\pi n_e - n_o}{\lambda} h \text{ for } k = 1, 2, \dots, N-1.$$

The transfer matrix relates the components of the complex electric vector V_k at the enter surface of the k layer

$$V_k = \begin{pmatrix} A_k + iB_k \\ C_k + iD_k \end{pmatrix}$$

to the complex electric vector V_{k+1} at the exit surface of the k layer

$$V_{k+1} = \begin{pmatrix} A_{k+1} + iB_{k+1} \\ C_{k+1} + iD_{k+1} \end{pmatrix}.$$

One obtains the following recurrence relations

$$\begin{aligned} A_{k+1} &= A_k \cos \alpha + (B_k \cos 2\phi'_k + D_k \sin 2\phi'_k) \sin \alpha \\ B_{k+1} &= B_k \cos \alpha - (A_k \cos 2\phi'_k + C_k \sin 2\phi'_k) \sin \alpha \\ C_{k+1} &= C_k \cos \alpha + (B_k \sin 2\phi'_k - D_k \cos 2\phi'_k) \sin \alpha \\ D_{k+1} &= D_k \cos \alpha - (A_k \sin 2\phi'_k - C_k \cos 2\phi'_k) \sin \alpha \end{aligned} \quad (10)$$

Since the component of the complex electric field when leave LC in the N^{th} layer is

$$V_N = \begin{pmatrix} A_N + iB_N \\ C_N + iD_N \end{pmatrix}$$

and its projection on the crossed analyzer is $C_N + iD_N$,

then the transmission is $T = C_N^2 + D_N^2$.

Light transmission for the three wavelengths of the light beam was thus computed as function of applied voltage with cell thickness, rubbing angle and anchoring energy at the command surface as parameters.

In Fig. 6 the experimental results are compared to those simulated for a cell thickness of $H = 1.73\mu\text{m}$ corresponding to $\delta_G = 0.597$ for the three wavelengths used in this study. The transmission curves for all these three wavelengths have a similar shape in the experimental case as well as in the simulated one. The only difference is a scale factor of the voltage $U_{Exp}/U_{Theor} = 1.608$. This difference is a consequence of the very simple model applied for simulation.

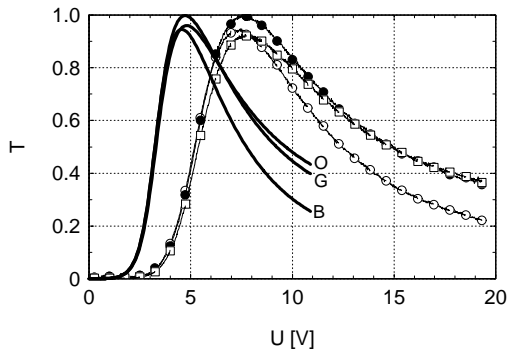


Fig. 6. Comparison of the experimental (\circ , \bullet , \square for the wavelength corresponding to B, G, O respectively) and simulated (B, G, O) results for the cell with optical thickness $\delta_G = 0.597$.

Minimizing the free energy only in the volume defined by the electrodes and the glass substrates ignores the interaction of the liquid crystal from this volume with that in the neighborhood over the electrodes as well as the electric field existent in this later region. The liquid crystal is distorted by the electric field either in the considered volume as well as in the adjacent space, involving higher voltage necessary to obtain a certain deformation level for the director field in the ID space. The liquid crystal distortion can be estimated within the region over the electrodes for a depth of minimum $0.3d$ on both sides of investigated zone. The electric field is nonuniform in the volume where the minimizing was performed; moreover there is a vertical component of it. Accordingly the director field is nonuniform in an horizontal plan and has a vertical component too. This contributes also to the observed differences between the experimental and calculated transmission curves as function of the voltage.

Despite the differences between the experimental and calculated results, using the scale factor $U_{Exp}/U_{Theor} = 1.608$ leads to a good concordance of the transmission curves. Therefore, the iso-transmission maps thus calculated might be useful to characterize from electro-optic point of view of the operating mode IPS.

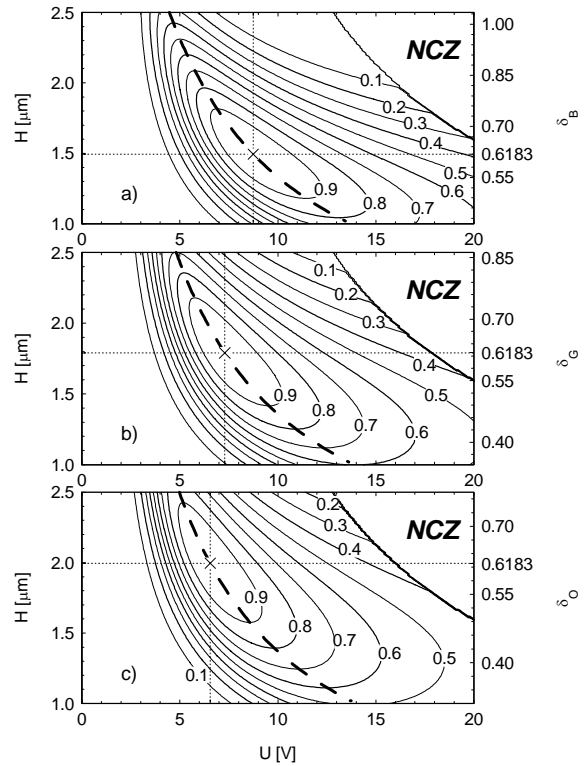


Fig. 7. Iso-transmission maps of the electro-optic effect as function of cell thickness H for the wavelength of a) 488 nm; b) 548 nm and c) 591 nm. NCZ stands for the non-calculated zone. The dashed lines correspond to the maximum transmission for a given thickness. Points having transmission $T = 1$ were marked by \times symbol.

In the Figs. 7 such iso-transmission curves are shown in dependence on the applied voltage U and on the thickness for wavelengths 488 nm, 548 nm and 591 nm respectively. The rubbing angle was 13° and anchoring was strong. The optical path difference δ_λ corresponding to the thickness of the LC layer is indicated on the right side of the corresponding figure. In all three cases the highest level of the transmission ($T=1$) was obtained for a thickness, which has an associated value of $\delta_\lambda = 0.6183$ in agreement with the experimental data. Dashed lines give the maximum values of the transmission for a given thickness, as well as the voltages needed to reach these values.

For a given rubbing angle we found that the optimum thickness and its associated δ_λ show a non-monotonous dependence of anchoring energy (Fig. 8). Taking into account that the anchoring energy depends on the nature of the LC, one can conclude that δ_λ has not the same value as was previously reported [11]. For a given anchoring energy the optimum thickness decreases with the increasing of the rubbing angle (Fig. 8).

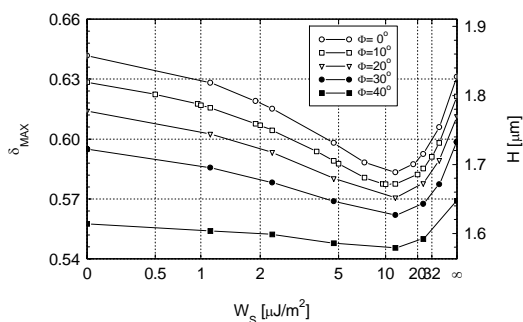


Fig. 8. Dependence of optimum thickness for different rubbing angles on the anchoring energy.

4. Conclusions

The optical transmission of an IPS liquid crystal cell was investigated as function of the thickness of the LC layer by using a specially designed cell. All the cell parameters except the thickness are thus kept constant allowing an easy comparison of the transmission data. A polyvinyl alcohol layer rubbed at 13° was used for alignment ensuring a strong LC anchoring.

The highest level of the transmission was obtained for a thickness, which has associated a value of optical pass difference $\delta_\lambda \sim 0.66$ greater than the value reported in the literature.

The curves of the optical transmission were simulated using a simple model. In the case of a strong anchoring and for a rubbing angle of 13° the highest level of the transmission was obtained for a thickness, which has associated a value of $\delta_\lambda = 0.6183$, in agreement with the experimental results.

Iso-transmission maps for different rubbing angles and different anchoring energies were calculated putting in evidence the electro-optic characteristics of the IPS operating mode.

For a given rubbing angle we found that the optimum thickness and its associated δ_λ show a nonmonotonous dependence on the anchoring energy. Because the anchoring energy depends on the nature of the LC, one can consider that δ_λ has not the same value for all the LCs contrary to the previously reported results.

For a given anchoring energy the optimum thickness decreases with the increasing of the rubbing angle.

Acknowledgement

Financial support from Romanian Ministry of Education and Research (Project CERES 4-26/C3) is gratefully acknowledged by the authors. In addition I. Z. expresses gratitude for the participation grant at the ECLC 2007 from the Project CEEEX ET 3175.

References

- [1] M. Oh-e, K. Kondo, Appl. Phys. Lett. **67**, 3895 (1995).
- [2] X. T. Li, A. Kowakami, H. Akiyama, S. Kobayashi, Y. Iimura, Jpn. J. Appl. Phys., **37**, L743 (1998).
- [3] D. Andrienko, F. Barbet, D. Bormann, Y. Kurioz, S.-B. Kwon, Y. Reznikov, M. Warengem, Liq. Cryst., **27**, 365 (2000).
- [4] Y. Sun, Z. Zhong, H. Ma, X. Zhu, S.-T. Wu, J. Appl. Phys., **93**, 3920 (2003).
- [5] Y. Sun, S.-T. Wu, Jpn. J. Appl. Phys., **42**, L 423 (2003).
- [6] R. Lu, X. Zhu, S.-T. Wu, Q. Hong, T. X. Wu, J. Display Technol., **1**, 3 (2005).
- [7] R. Lu, Q. Hong, Z. Ge, S.-T. Wu, Optics Lett., **14**, 6243 (2006).
- [8] Z. Ge, X. Zhu, T. X. Wu, S.-T. Wu, J. Display Technol., **2**, 114 (2006).
- [9] B. S. Jung, I. S. Baik, I. S. Song, G.-D. Lee, S. H. Lee, Liq. Cryst., **33**, 1077 (2006).
- [10] C. Yen Hung, C. T. Hsieh, J. R. Tian, Optics Lett., **14**, 9931 (2006).
- [11] G. Rong-Hua, S. Yu-Bao, K. Wen-Xiu, Liq. Cryst., **33**, 829 (2006).
- [12] G. Rong-Hua, K. Wen-Xiu, S. Yu-Bao, Liq. Cryst., **34**, 467 (2007).
- [13] a) S.-T. Wu, J. Appl. Phys., **69**, 2080 (1991); b) BDH Data sheets.
- [14] G.-P. Chen, H. Takezoe, A. Fukuda, Liq. Cryst. **5**, 341 (1989).
- [15] Atomerigic Chemetals Corp. Data Sheets.
- [16] R. Jones, J. Opt. Soc. Am., **31**, 488 (1941).
- [17] P. Yeh, C. Gu, Optics of Liquid Crystal Displays, Wiley-InterScience: New York, (1999).

*Corresponding author: frunza@infim.ro